Quenching of $I(^2P_{1/2})$ by NO_2, N_2O_4, and N_2O

Md. Humayun Kabir, Valeriy N. Azyazov,† and Michael C. Heaven*

Department of Chemistry, Emory University, Atlanta, Georgia 30322

Received: May 29, 2007; In Final Form: July 27, 2007

Quenching of excited iodine atoms ($I(5p^5, {}^2P_{1/2})$) by nitrogen oxides are processes of relevance to discharge-driven oxygen iodine lasers. Rate constants at ambient and elevated temperatures (293−380 K) for quenching of $I(^2P_{1/2})$ atoms by NO_2, N_2O_4, and N_2O have been measured using time-resolved $I(^2P_{1/2}) \rightarrow I(^2P_{3/2})$ 1315 nm emission. The excited atoms were generated by pulsed laser photodissociation of CF_3I at 248 nm. The rate constants for $I(^2P_{1/2})$ quenching by NO_2 and N_2O were found to be independent of temperature over the range examined with average values of $(2.9 \pm 0.3) \times 10^{-15}$ and $(1.4 \pm 0.1) \times 10^{-15}$ cm^3 s^{-1}, respectively. The rate constant for quenching of $I(^2P_{1/2})$ by N_2O_4 was found to be $(3.5 \pm 0.5) \times 10^{-13}$ cm^3 s^{-1} at ambient temperature.

Introduction

Carroll et al.[1] were the first to demonstrate an oxygen−iodine laser (OIL) that utilizes an electric discharge to produce singlet oxygen molecules $O_2(a^1\Delta_g)$. One of the distinguishing features of discharge-driven singlet-oxygen generators is that a substantial quantity of $O(^3P)$ is produced along with $O_2(a^1\Delta_g)$. It has been shown[2−5] that $O(^3P)$ is detrimental to the laser due to the fast quenching process

$$I(^2P_{1/2}) + O(^3P) \rightarrow I(^2P_{3/2}) + O(^3P) \quad (1)$$

Recent determinations of the rate constant for this deactivation channel have established a value of $k_1 = (1.2 \pm 0.2) \times 10^{-11}$ cm^3 s^{-1} (refs 2 and 6−8). In the following, $I(^2P_{1/2})$, $I(^2P_{3/2})$, and $O_2(a^1\Delta_g)$ are designated by I*, I, and $O_2(a)$, respectively.

Reaction 1 results in a significant loss of I* for typical discharge-generated oxygen-atom concentrations. Due to the rapidly established equilibrium between I* and $O_2(a)$

$$I + O_2(a) \leftrightarrow I^* + O_2 \quad (2)$$

quenching of I* also results in deactivation of $O_2(a)$. Working with prototype electrically driven oxygen-iodine laser (EOIL) systems, Carroll et al.[3] and Rawlins et al.[2] found that production of I* was increased when NO_2 was added to the postdischarge flow upstream of the iodine injection. They concluded that this effect was due to consumption of the excess oxygen atoms via the process

$$O(^3P) + NO_2 \rightarrow O_2 + NO \quad (3)$$

($k_3 = (9.5 \pm 1.1) \times 10^{-12}$ cm^3 s^{-1}, ref 9). The optimal concentration of NO_2 to be added to the flow is dependent, among other factors, on the rate constant for the quenching of I* by NO_2

$$I^* + NO_2 \rightarrow I + NO_2 \quad (4)$$

As NO_2 readily forms the N_2O_4 dimer, the quenching process

$$I^* + N_2O_4 \rightarrow I + N_2O_4 \quad (5)$$

is also a matter for concern. There is only one report of an attempt to measure the rate constant for reaction 4. Han et al.[4] obtained an upper bound at room temperature of $k_4 < 8.5 \times 10^{-14}$ cm^3 s^{-1}.

In order to determine an accurate value for the rate constant for deactivation of I* by NO_2, we reinvestigated this process at ambient temperature and extended our measurements to elevated temperatures. The temperature dependence study was motivated by two factors. First, the conditions in EOIL devices span a wide temperature range as the gas mixture travels from the discharge to the optical cavity. Immediately after discharge the gas temperature can be greater than 700 K. Cooling to temperatures below 300 K by the time the gas reaches the cavity is desirable as this increases the gain (due to the effect of temperature on the equilibrium represented by reaction 2). Second, the equilibrium between NO_2 and N_2O_4 is temperature dependent, and measurements made over a range of temperatures were helpful in separating out the quenching contributions from reactions 4 and 5.

Quenching of I* by N_2O was studied both for fundamental reasons and because of the relevance to a particular type of photolytically driven oxygen−iodine laser. Zolotarev et al.[10] explored a laser scheme where photolysis of O_3 was used as the primary source of $O_2(a)$. In attempts to improve the performance of this system, Zolotarev et al.[10] tested the use of N_2O, N_2, and/or CO_2 as reagents for removal of the unwanted $O(^1D)$ photoproduct. The best results were obtained for N_2O, and Zolotarev et al.[11] concluded that an increase in laser power was achieved due to the fact that N_2O consumes oxygen atoms in processes

$$O(^1D) + N_2O \rightarrow NO + NO \quad (6a)$$

$$\rightarrow O_2(a\ ^1\Delta_g, X^3\Sigma^-_g) + N_2 \quad (6b)$$

* To whom correspondence should be addressed. E-mail: mheaven@emory.edu.

† Visiting scientist from the Samara Branch of the P. N. Lebedev Physics Institute.

10.1021/jp0741511 CCC: $37.00
Published on Web 09/14/2007

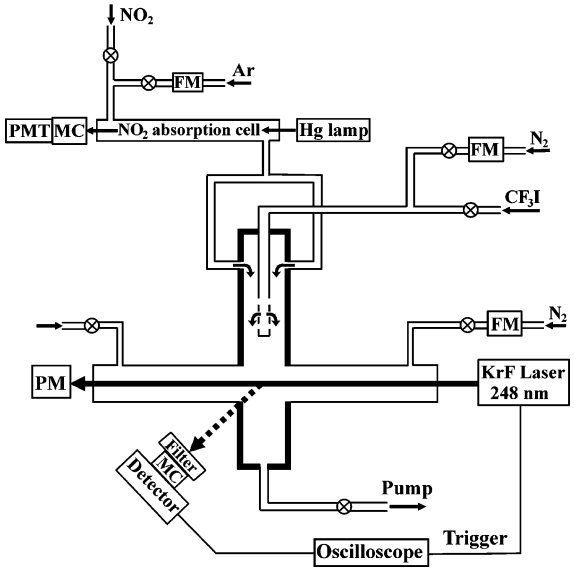

Figure 1. Schematic diagram of the experimental setup for I* quenching measurements. PMT, photomultiplier tube; MC, monochromator; detector, liquid nitrogen cooled germanium photodetector coupled with a preamplifier; FM, flow meter; PM, power meter.

where $O_2(a)$ is the dominant product of reaction 6b. Recently[7] the branching fraction of electronically excited O_2 produced by channel 6b was found to be >0.9. The optimal mole fraction of N_2O for the laser driven by O_3 photolysis depends on the rate at which I* is quenched by N_2O

$$I^* + N_2O \rightarrow I + N_2O \qquad (7)$$

Han et al.[12] reported a rate constant for reaction 7 at room temperature of $k_7 = 2.1 \times 10^{-15}$ cm^3 s^{-1}. This measurement, made using photolysis of CF_3I/N_2O mixtures at 266 nm, was approximately consistent with the results of Hathorn et al.,[13] who obtained a value of $k_7 = (1.3 \pm 0.2) \times 10^{-15}$ cm^3 s^{-1}. In the present work we extended the characterization of reaction 7 by performing the first measurements at elevated temperatures.

Experimental Methods

Pulsed laser photolysis and emission spectroscopy techniques were used to measure the rate constants. The apparatus used for these experiments is shown in Figure 1. The photolysis cell was constructed from a solid brass block with 1 cm diameter channels for the flow of gases, passage of the photolysis laser beam, and observation of infrared emissions from the photolysis zone. To reduce window scattering problems for the photolysis beams, two baffle arms (35 cm long) were attached to the photolysis cell. UV-grade fused silica windows were attached to the ends of both arms. Sets of apertures were mounted inside the baffle arms. Emission from the photolysis products was recorded at right angles to the axis of the laser beam via a quartz window. The temperature in the photolysis zone was measured by a beaded wire thermocouple placed at the exit of the photolysis zone.

A flow of CF_3I vapor was added to a N_2 carrier flow, and the mixture was admitted into the photolysis cell through a sliding injector. An NO_2/Ar mixture was injected through two opposing inlets connected to the main gas channel. Mixing of the gases, CF_3I/N_2 and NO_2/Ar, occurred during their transport to the photolysis zone. A continuous and small flow of N_2 (200 mL/min) was introduced in the baffle arms through gas inlet ports to protect the windows from the photoproducts. The cell was evacuated by a rotary pump, and flow rates were chosen such that the total pressure in the photolysis cell was about ~90 Torr. This pressure was used to provide rapid relaxation of the translation energy of the photofragments and limit diffusion. All experiments were performed with a gas flow velocity of about 112 cm/s. The partial pressures of the gases were determined from the photolysis cell pressure and the measured flow rates of the various gases. The flow rates were controlled using electronic mass-flow meters (Omega FMA 1814) and needle valves.

The NO_2 partial pressure in the flow cell was varied from 0.5 to 8.0 Torr. The NO_2 concentration was measured by an optical absorption method as well as by the increase in the flow cell pressure upon addition of the NO_2 flow. As shown in Figure 1, a 53 cm long optical cell was used for the absorption measurement. The 365 nm light from a low-pressure mercury lamp was monitored. A 0.25 m monochromator was used to select this spectral line, and the transmitted intensity was recorded by a photomultiplier/picoammeter combination. For the conditions of these experiments the concentration of NO_2 greatly exceeded that of N_2O_4, such that the optical absorption measurements were not significantly influenced by the presence of the latter. Gas pressures in the absorption and photolysis cells were measured using capacitance manometers (MKS Baratron model 122A, 0-100 Torr).

The photolysis laser was a Lambda-Physik Compex Pro 102 excimer laser operating at a wavelength of 248 nm (KrF, pulse duration 10 ns). A pulse repetition rate of 5 Hz was used, which was slow enough to ensure that a fresh sample of gas was photolyzed on each pulse. The laser power was adjusted to provide fluences of $E = 3.5-18$ mJ/cm^2 in the center of the photolysis cell. Excitation of CF_3I at 248 nm induces the processes

$$CF_3I + h\nu\,(248\text{ nm}) \rightarrow CF_3 + I \qquad (8a)$$

$$\rightarrow CF_3 + I^* \qquad (8b)$$

with a branching ratio of 0.11:0.89 in favor of I* production.[14] In order to measure the I* → I emission decay profiles at 1315 nm, a monochromator (0.2 m), long-pass filter, and fast germanium detector (ADC model 403 HS, detector area 25 mm^2) were arranged linearly and placed in front of the observation window of the photolysis cell. A long-pass filter was used to minimize the scattered light from the photolysis laser. Time-resolved I* emission decay signals from the germanium detector were averaged for 64 laser pulses and stored using a digital oscilloscope (Yokogawa DL 1520, 150 MHz bandwidth).

For measurements involving CF_3I/N_2O mixtures the photolysis cell was operated without carrier gases and the window purge flows were not used. Otherwise, the pumping rate was kept the same as it was for the NO_2/Ar/CF_3I/N_2 experiments. Partial pressures of N_2O in the photolysis cell were varied from 10 to 100 Torr.

The sample gases NO_2 (>99.5%), N_2O (UHP, 99.99%), Ar (UHP, 99.998%), and N_2 (UHP, 99.998%) were used without further purification. The trifluoromethyl iodide, CF_3I (stated purity > 99%), contained I_2 as a significant impurity. As the quenching of I* by I_2 is very fast (3.8×10^{-11} cm^3 s^{-1}),[15] it was important to reduce the level of this contaminant. CF_3I was purified by degassing and trap-to-trap distillation using an ethanol/dry ice slush bath to condense the I_2.

Results and Discussion

I* + NO_2 Quenching. Several complications were encountered in studying the quenching of I* by NO_2. As noted above, the N_2O_4 dimer is present in equilibrium with NO_2

$$NO_2 + NO_2 + M \leftrightarrow N_2O_4 + M \quad (9)$$

The partial pressure, $P(N_2O_4)$, depends on the total pressure $P_o = P(N_2O_4)+P(NO_2)$ and the temperature T according to the expression

$$P(N_2O_4) = P_0 + K_{eq}/2 - \sqrt{K_{eq}(P_0 + K_{eq}/4)} \quad (10)$$

where $P(NO_2)$ is the partial pressure of NO_2 and K_{eq} is the equilibrium constant. The latter is given by $K_{eq} = P(NO_2)^2/P(N_2O_4) = 760 \exp(21.13-6880/T)$ (in units of Torr, ref 16). Note that the fraction of N_2O_4 in the mixture decreases as the total pressure is reduced and/or the temperature is increased. These trends have been used to disentangle the rate constants for quenching of I* by NO_2 and N_2O_4.

A second complication is that 248 nm light photodissociates both NO_2 and N_2O_4 to yield oxygen atoms[17−20]

$$NO_2 + h\nu\,(248\text{ nm}) \rightarrow NO + O(^3P) \quad (11)$$

$$N_2O_4 + h\nu\,(248\text{ nm}) \rightarrow NO_2(A^2B_2) + NO_2(B^2B_1) \quad (12a)$$

$$\rightarrow NO + O(^3P) + NO_2 \quad (12b)$$

Under our experimental conditions the $O(^3P)$ atoms were quickly converted into oxygen molecules by reaction 3. Molecular oxygen deactivates I* via

$$I^* + O_2 \rightarrow I + O_2(a) \quad (13)$$

with a rate constant of $k_{13} = 2.7 \times 10^{-11}$ cm^3 s^{-1} (ref[15]).

Another possible complication is that the CF_3 radical formed in process 8 is reactive toward NO_2, leading to formation of various products[21−23] that may also physically or chemically quench I*

$$CF_3 + NO_2 \rightarrow CF_2O + FNO \quad (14a)$$

$$\rightarrow CF_2O + F + NO \quad (14b)$$

$$CF_3 + NO_2 + M \rightarrow CF_3NO_2 + M \quad (14c)$$

Oum et al.[22] studied the $CF_3 + NO_2$ reaction using time-resolved FTIR emission spectroscopy and observed reaction channels 14a and 14b. They estimated the relative branching ratio of reactions 14a to 14b to be 1:0.015. As described below, care was taken to minimize the influence of these complications on the accuracy of our measurements.

Typical decay profiles for the I* emission are shown in Figure 2. These traces were recorded at room temperature. The partial pressure of $NO_2 + N_2O_4$ was varied, while the total pressure within the photolysis cell was held constant at 90 Torr by simultaneous adjustment of the buffer gas flow. The initial spike observed in the decay profiles was due to emissions from short-lived excited states species (e.g., UV excitation of the impurity I_2). Beyond this artifact, the emission profiles exhibited single-exponential decay characteristics. In the absence of NO_2 (curve *1*), the I* emission decay rate was primarily determined by the residual I_2. Quenching of I* by CF_3I is known to be inefficient with a rate constant of $(3.5 \pm 0.6) \times 10^{-16}$ cm^3 s^{-1} (ref 24).

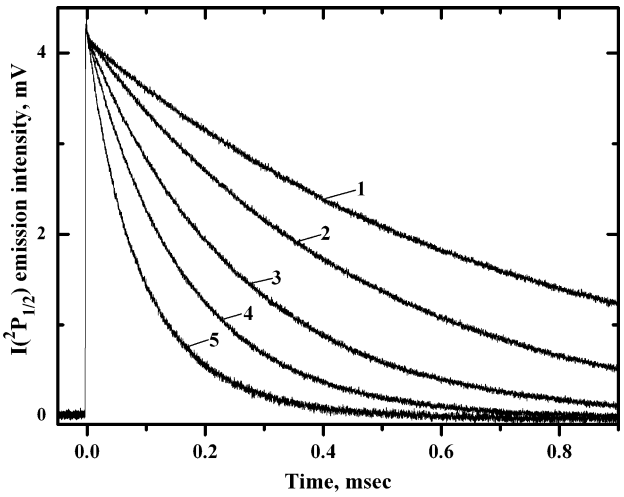

Figure 2. Time-resolved I* → I emission decay profiles recorded from the pulsed laser photolysis (248 nm) of $NO_2/N_2O_4/Ar/CF_3I/N_2$ mixtures at ambient temperature, $P_{tot} = 90$ Torr, $E = 3.5$ mJ/cm^2, $P(CF_3I) = 0.1$ Torr. These traces illustrate the dependence of the signal on the $NO_2 + N_2O_4$ pressure P_0: *(1)* 0, *(2)* 2.1, *(3)* 3.9, *(4)* 5.7, and *(5)* 8 Torr.

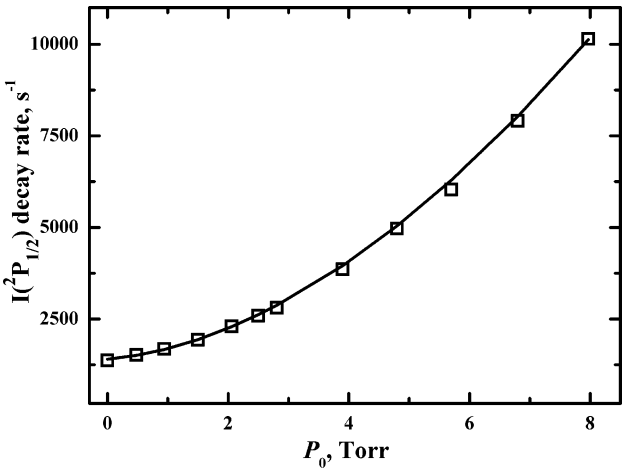

Figure 3. Decay rates for I* as a function of $P_0 = P(NO_2) + P(N_2O_4)$. Photolysis conditions: laser pulse fluence $E = 3.5$ mJ/cm^2, $P_{tot} = 90$ Torr, $P(CF_3I) = 0.1$ Torr, $T = 293$ K.

The decay rate obtained using CF_3I as supplied was considerably faster than would be expected on the basis of a 1% impurity of I_2. Using trap-to-trap distillation of CF_3I we were able to reduce I_2 to the point where the I* decay rate was consistent with a 1% impurity level. Fluorescence decay rates were extracted from curves such as those shown in Figure 2 by nonlinear least-squares fitting with the data for the first 5 μs of the signal omitted.

The I* fluorescence decay rates are plotted as a function of the sum of the $NO_2 + N_2O_4$ partial pressures in Figure 3. This plot shows an obviously nonlinear dependence of the decay rate on P_0. The functional form of this dependence could be explained by assuming that quenching by N_2O_4 (or a photoproduct from N_2O_4) was much faster than quenching by NO_2. This hypothesis was tested by repeating the measurements at higher temperatures. Equation 10 predicts that the mole fraction of N_2O_4 will decrease rapidly with increasing temperature. For example, for $P_0 = 8$ Torr the partial pressure of N_2O_4 is 0.73 and 0.02 Torr at 293 and 350 K, respectively. Heating the apparatus reduced the fluorescence decay rates at the higher pressures, and curvature of the Stern−Volmer plots (decay rate

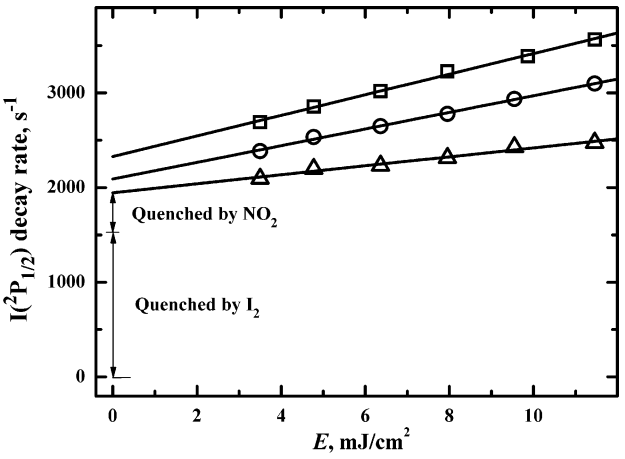

Figure 4. I* quenching decay rates as a function of laser pulse fluence E at $T = 353$ K and $P(CF_3I) = 0.1$ Torr for NO_2 partial pressures: (□) 6, (○) 4, and (Δ) 2 Torr. Solid lines were obtained from linear least-squares analyses. Vertical arrows indicate the decay rates resulting from quenching by NO_2 and I_2 at $E = 0$ for the 2 Torr data.

vs P_0) was not observed for $P_0 \leq 8$ Torr when the temperature was above 350 K.

Although the Stern−Volmer plots for $T \geq 350$ K were linear, they were still influenced by quenching contributions from the photoproducts. To remove this effect, the dependence of the decay rates on the laser fluence was characterized. Figure 4 shows plots of the decay rates vs the laser fluence for three different values of P_0. Here it can be seen that the decay rates increased with the laser power, as would be expected if some of the photoproducts were rapid quenchers of I* (e.g., O and O_2). Extrapolation of these plots to zero laser fluence gives the decay rate in the absence of quenching contributions from photoproducts. As the I* radiative decay rate is comparatively slow (8 s^{-1}), the zero fluence intercept was determined by the sum of the I_2 and NO_2 quenching rates. For each series of measurements the decay curve with $P_0 = 0$ was recorded to establish the I_2 quenching rate. This was subtracted from subsequent measurements with $P_0 > 0$ to provide the NO_2 quenching rates. Stern−Volmer plots constructed using the corrected data are shown in Figure 5. Here it can be seen that the rate constant for quenching by NO_2 did not exhibit a measurable dependence on temperature over the range from 353 to 381 K. A temperature-independent rate constant of $k_4 = (2.9 \pm 0.3) \times 10^{-15}$ cm^3 s^{-1} was obtained by averaging three sets of measurements of k_4 made at temperatures within the range 353−381 K. In considering the photochemical products that could be responsible for the laser power dependence of the decay rates, it is of interest to examine the quenching resulting from photochemically generated O and O_2. The absorption cross-section for NO_2 at 248 nm is 1.6×10^{-20} cm^2 (ref 25), and the branching fraction for production of O atoms is unity. For a NO_2 pressure of 6 Torr and a laser fluence of 7 mJ cm^{-2} the concentration of promptly formed O atoms is predicted to be 2.7×10^{13} cm^{-3}. Reaction 3 then converts the O atoms to O_2 at a rate of 2×10^6 s^{-1}, which is fast compared to the observed fluorescence decay rate (≈3000 s^{-1}, cf., Figure 4). Quenching of I* by the product O_2 then occurs at a rate of about 730 s^{-1}, which is sufficient to account for all of the effect of laser power on the decay rates. Apparently, quenching by O_2 dominated over the quenching contributions of the other photochemical products.

$I(^2P_{1/2}) + N_2O_4$ Quenching at Ambient Temperature. The curved Stern−Volmer plot observed at room temperature (Figure 3) could be interpreted in terms of enhanced quenching caused by N_2O_4 or a photoproduct of N_2O_4. The absorption cross section

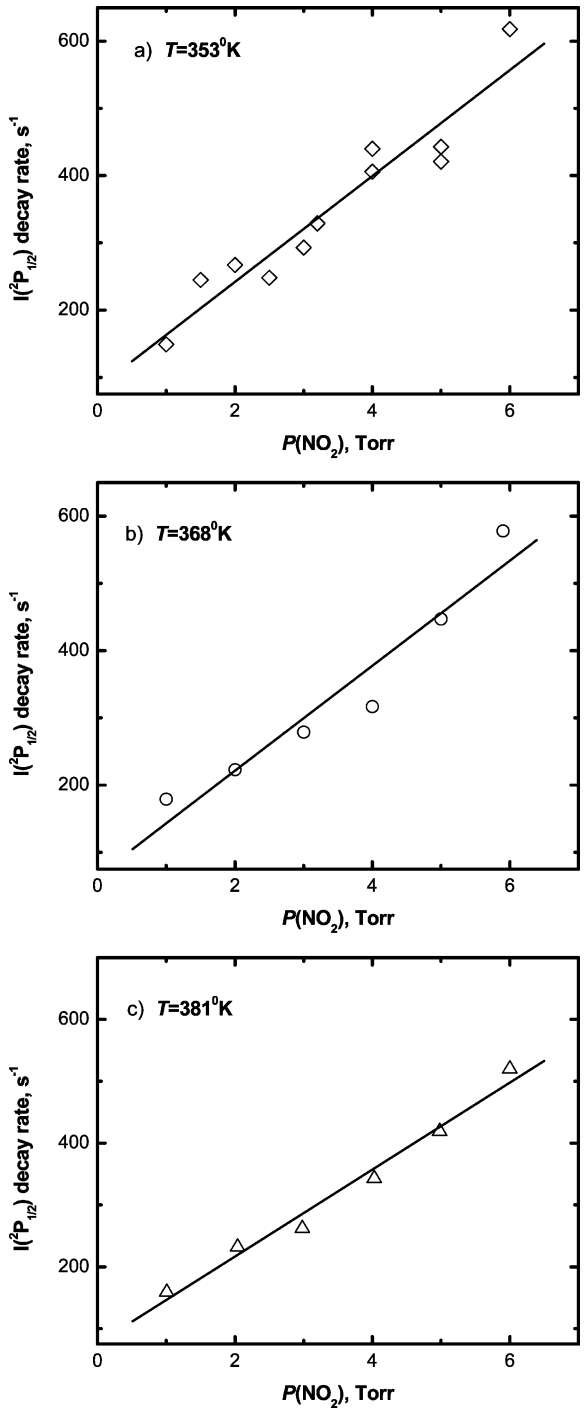

Figure 5. Dependence of the I* decay rate on the NO_2 pressure from data obtained at three different temperatures over the range 353−381 K. These measurements were made with $E = 3.5$ mJ/cm^2 and $P(CF_3I) = 0.1$ Torr. The lines were obtained from linear least-squares analyses.

of N_2O_4 at 248 nm is a factor of 80 greater than that of the monomer.[19] Hence, O atoms from process 12b might be involved in the quenching kinetics. As noted above, the conditions of these experiments are such that the O atoms are rapidly converted to O_2 by reaction 3. Photolysis of N_2O_4 by 248 nm light has been examined by Morrell et al.[19] They estimated that the yield for O-atom production was no more than $\eta_{12b} \approx 0.2$. Assuming the upper bound value, the concentration of O atoms produced by photolysis is given by

$$[O] \approx 5.1 \times 10^{13} \eta_{12b} P(N_2O_4) E \qquad (15)$$

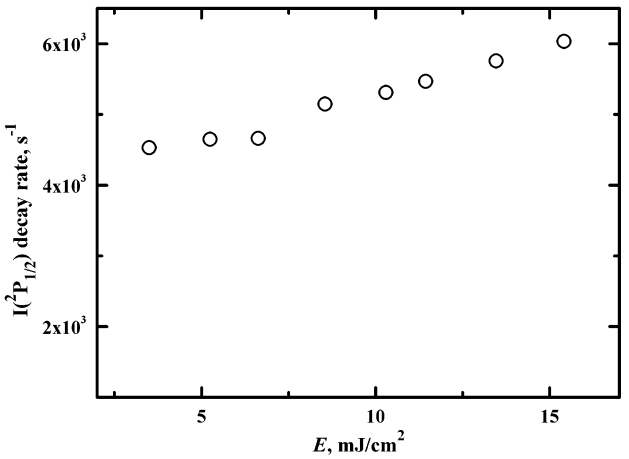

Figure 6. Dependence of the I* decay rates on the laser pulse fluence for $P_{tot} = 90$ Torr, $P(NO_2) = 4.1$ Torr, $P(CF_3I) = 0.1$ Torr, $T = 293$ K.

where [O] is in atoms cm^{-3}, $P(N_2O_4)$ is in Torr, and E is in mJ cm^{-2}. Consider an experiment with $P_0 = 8$ Torr and $E = 3.5$ mJ cm^{-2}. At room temperature the partial pressure of N_2O_4 will be 0.73 Torr (eq 10) and photolysis yields [O] $= 2.6 \times 10^{13}$ cm^{-3}. If the atoms are all converted to O_2, this will result in a photoproduct quenching rate, $k_{13}[O_2]$ of 730 s^{-1}. This is an order of magnitude smaller than the decay rate observed under these conditions (cf. Figure 3). Further evidence that photolysis of N_2O_4 was not important in the room-temperature quenching kinetics was obtained by examining the decay rate as a function of laser power for $P_0 = 4$ Torr. These data, shown in Figure 6, were consistent with the results from measurements at elevated temperatures (cf. Figure 4), where the partial pressure of N_2O_4 was considerably lower.

On the basis of the above arguments, it was concluded that the curvature of the plot in Figure 3 was the result of quenching by N_2O_4. To extract the rate constants for reactions 4 and 5, the decay rate data (Γ) of Figure 3 were fitted to the expression

$$\Gamma = \Gamma_0 + k_4[NO_2] + k_5[N_2O_4] \qquad (16)$$

where Γ_0 is the decay rate with $P_0 = 0$ and the number densities for NO_2 and N_2O_4 were derived from eq 10 and the ideal gas law. The smooth curve in Figure 3 shows the results for the fit, which yields values for the rate constants of $k_4 = (2.8 \pm 1.1) \times 10^{-15}$ cm^3 s^{-1} and $k_5 = (3.45 \pm 0.11) \times 10^{-13}$ cm^3 s^{-1}. The quoted error ranges are one standard deviation for the fitted parameters. The large error range for k_4 that was obtained in this fit was a consequence of the strong correlation between the parameters. Fitting with k_4 fixed at the value obtained from the higher temperature measurements (2.9×10^{-15} cm^3 s^{-1}) yielded $k_5 = (3.45 \pm 0.03) \times 10^{-13}$ cm^3 s^{-1}. Given the uncertainties in determination of the N_2O_4 concentration, we estimate that a conservative error range for k_5 is $(3.5 \pm 0.5) \times 10^{-13}$ cm^3 s^{-1}. The value of k_5 reported here was derived from the single set of data shown in Figure 3.

$I(^2P_{1/2})$ + N_2O Quenching Process. Photolysis of CF_3I in the presence of N_2O was used to examine the quenching of I* by N_2O. As the absorption cross section for N_2O at 248 nm is extremely small, there were no photochemical complications associated with these experiments. N_2O partial pressures in the range of 10−100 Torr were used in order to observe a well-defined quenching effect, and data were recorded at the temperatures 293, 317, 335, 357, and 378 K. Figure 7 shows Stern−Volmer plots for data recorded over the entire temperature range. Linear quenching plots were expected, but three of the data sets show a slight curvature for the lowest pressure points. We do not have an explanation for this behavior at present, but we suspect that it is an experimental artifact. Linear fits to the data yield rate constants (10^{-15} cm^3 s^{-1}) of 1.39 ± 0.03 (293 K), 1.40 ± 0.04 (317 K), 1.27 ± 0.02 (335 K), 1.36 ± 0.05 (357 K), and 1.31 ± 0.03 (378 K). These data indicate that the quenching rate constant is effectively independent of temperature over the range studied and can be represented by the value $k_7 = (1.4 \pm 0.1) \times 10^{-15}$ cm^3 s^{-1}.

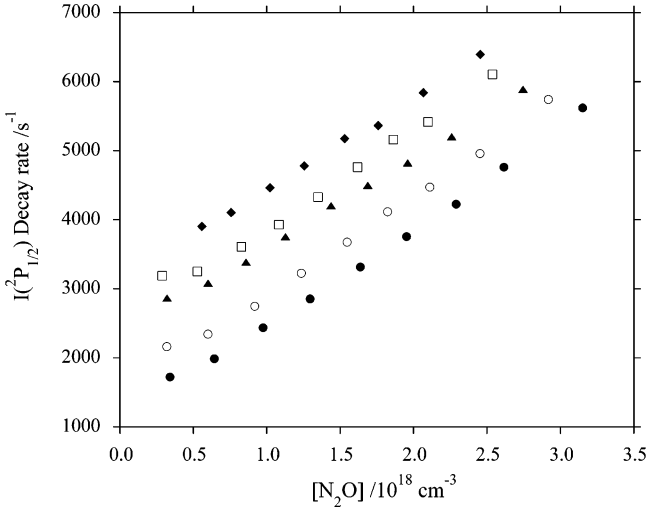

Figure 7. I* decay rates as a function of $P(N_2O)$. Photolysis conditions: $E = 3.5$ mJ/cm^2, $P(CF_3I) = 0.1$ Torr. The data shown were taken at temperatures of 293 (●), 317 (○), 335(▲), 357 (□), and 378 K (♦). Note that the data have been separated for clarity by shifting along the decay rate axis. The unshifted data points are extensively overlapped.

Discussion

The present measurement of the room-temperature rate constant for quenching of I* by N_2O is in good agreement with the value reported by Hathorn et al.[13] ($(1.3 \pm 0.2) \times 10^{-15}$ cm^3 s^{-1}). The dependence of this rate constant on the temperature was too weak to be determined, indicating that the mechanism does not involve a barrier or facilitation through formation of a long-lived collision complex. The rate constant for quenching by NO_2 was well below the upper bound reported by Han et al.[4] In that earlier study the limiting factor was the presence of impurity O_2 in the NO_2 sample. The results obtained in this study indicate that the I* quenching characteristics of N_2O and NO_2 are quite similar. This is an interesting observation that deserves some further consideration.

The quenching rate constants (293 K) for NO (ref 26), NO_2, and N_2O are 1.2×10^{-13}, 2.9×10^{-15}, and 1.4×10^{-15} cm^3 s^{-1}, respectively. NO and NO_2 are open-shell species. Their interactions with iodine are such that INO and INO_2 are moderately stable molecules.[27,28] In contrast, N_2O is a closed-shell molecule that interacts with I via weak van der Waals forces. Hence, the large difference in the quenching rate constants for NO and N_2O is not surprising, but the low efficiency for quenching by NO_2 (compared to NO) was unexpected. It appears that long-range attractive forces facilitate quenching by NO, as Deakin and Husain[29] reported a negative temperature dependence for this process (and they speculated that transient formation of INO was implicated). Grimley and Huston[26] further suggested that quenching was mediated by means of seams of intersection occurring between the potential-

energy surfaces that correlate with the I* + NO and I + NO dissociation asymptotes.

INO_2 is bound, and it is reasonable to expect that one or two of the surfaces that correlate with I* + NO_2 will also possess potential minima. However, the slow quenching of I* by NO_2 indicates that intersections between the I* + NO_2 and I + NO_2 potential-energy surfaces do not occur within the energy range that is thermally accessible to collisions at $T \leq 380$ K. The small and similar quenching rate constants for NO_2 and N_2O suggest that they deactivate I* by an energy-transfer mechanism that does not involve potential surface intersections.

Quenching of I* by N_2O_4 was found to be a factor of 120 times more efficient than quenching by the monomer. Here it is of interest to note that the energy carried by I* (7603 cm^{-1}) exceeds the O_2N-NO_2 bond energy of about 4600 cm^{-1} (ref 20). Consequently, the channels

$$I^* + N_2O_4 \rightarrow I + NO_2 + NO_2 \quad (17a)$$

$$\rightarrow INO_2 + NO_2 \quad (17b)$$

could account for the faster deactivation by the dimer.

With regard to the discharge-driven oxygen−iodine laser, the quenching rate constant data indicate that both NO and NO_2 are relatively inefficient quenchers of I*. Their successful use as O-atom scavengers has been demonstrated in low-pressure laser systems, where the partial pressure of the NO or NO_2 added to the flow has been below 0.5 Torr. The quantity of NO or NO_2 that can be tolerated in the laser depends on both the partial pressures and the gas transit time between the I_2 injectors and the optical cavity. The rate constants provided by this study will facilitate further modeling for the design of higher power lasers, which will need to operate with much higher reagent densities than the devices explored to date.

Acknowledgment. We are grateful to W. Solomon and D. Carroll (CU Aerospace), S. Davis and T. Rawlins (PSI, Inc.), and G. Perram (AFIT) for many helpful discussions concerning the kinetics of oxygen discharges and discharge-driven iodine laser systems. This work was supported by the Air Force Office of Scientific Research through a Multidisciplinary Research Initiative (grant F49620-01-1-0357).

References and Notes

(1) Carroll, D. L.; Verdeyen, J. T.; King, D. M.; Zimmerman, J. W.; Laystrom, J. K.; Woodard, B. S.; Benavides, G. F.; Kittell, K.; Stafford, D. S.; Kushner, M. J.; Solomon, W. C. *App. Phys. Lett.* **2005**, *86*, 111104/1.
(2) Rawlins, W. T.; Lee, S.; Kessler, W. J.; Davis, S. J. *Appl. Phys. Lett.* **2005**, *86*, 051105.
(3) Carroll, D. L.; Verdeyen, J. T.; King, D. M.; Zimmerman, J. W.; Laystrom, J. K.; Woodard, B. S.; Benavides, G. F.; Kittell, K. W.; Solomon, W. C. *IEEE J. Quantum Electron.* **2005**, *41*, 213.
(4) Han, J.; Tinney, S. P.; Heaven, M. C. *Proc. SPIE* **2004**, *5448*, 261.
(5) Zolotarev, V. A.; Ishkov, D. V.; Podmar'kov, Y. P.; Frolov, M. P.; Yuryshev, N. N. *Sov. J. Quantum Electron* **1991**, *21*, 826.
(6) Azyazov, V. N.; Antonov, I. O.; Heaven, M. C. *J. Phys. Chem. A* **2007**, *111*, 3010.
(7) Azyazov, V. N.; Kabir, M. D.; Antonov, I. O.; Heaven, M. C. *J. Phys. Chem. A* **2007**, *111*, 6592.
(8) Palla, A. D.; Carroll, D. L.; Verdeyen, J. T.; Solomon, W. C. *J. Appl. Phys.* **2006**, *100*, 023117.
(9) Bemand, P. P.; Clyne, M. A. A.; Watson, R. T. *J. Chem. Soc., Faraday Trans. 2* **1974**, *70*, 564.
(10) Zolotarev, V. A.; Kryukov, P. G.; Podmar'kov, Y. P.; Frolov, M. P.; Yuryshev, N. N. *Sov. J. Quantum Electron.* **1989**, *19*, 709.
(11) Zolotarev, V. A.; Kryukov, P. G.; Podmar'kov, Y. P.; Frolov, M. P.; Yuryshev, N. N. Manufacture of singlet oxygen; (P.N. Lebedev Physics Institute, Moscow, USSR). Application SU #1668288 A1, 1991.
(12) Han, J.; Komissarov, A. V.; Tinney, S. P.; Heaven, M. C. *Proc. SPIE* **2003**, *4971*, 45.
(13) Hathorn, F. G. M.; Husain, D. J. *Trans. Faraday Soc.* **1969**, *65*, 2678.
(14) Fleder, P. *Chem. Phys.* **1991**, *155*, 435.
(15) Perram, G. P. *Int. J. Chem. Kinet.* **1995**, *27*, 817.
(16) Leenson, I. A. *J. Chem. Educ.* **2000**, *77*, 1652.
(17) Brouard, M.; Cireasa, R.; Clark, A. P.; Preston, T. J.; Vallance, C. *J. Chem. Phys.* **2006**, *124*, 064309/1.
(18) Hancock, G.; Morrison, M. *Mol. Phys.* **2005**, *103*, 1727.
(19) Morrell, C.; Breheny, C.; Haverd, V.; Cawley, A.; Hancock, G. *J. Chem. Phys.* **2002**, *117*, 11121.
(20) Sisk, W. N.; Miller, C. E.; Johnston, H. S. *J. Phys. Chem.* **1993**, *97*, 9916.
(21) Breheny, C.; Hancock, G.; Morrell, C. *Phys. Chem. Chem. Phys.* **2000**, *2*, 5105.
(22) Oum, K. W.; Hancock, G. *J. Phys. Chem. A* **1997**, *101*, 2634.
(23) Sugawara, K.; Nakanaga, T.; Takeo, H.; Matsumura, C. *J. Phys. Chem.* **1989**, *93*, 1894.
(24) Husain, D.; Wiesenfeld, J. R. *Trans. Faraday Soc.* **1967**, *63*, 1349.
(25) Vandaele, A. C.; Hermans, C.; Simon, P. C.; Carleer, M.; Colin, R.; Fally, S.; Merienne, M. F.; Jenouvrier, A.; Coquart, B. *J. Quant. Spectrosc. Radiat. Transfer* **1998**, *59*, 171.
(26) Grimley, A. J.; Houston, P. L. *J. Chem. Phys.* **1978**, *68*, 3366.
(27) Forte, E.; Hippler, H.; Van den Bergh, H. *Int. J. Chem. Kinet.* **1981**, *13*, 1227.
(28) Tucceri, M. E.; Dillon, T. J.; Crowley, J. N. *Phys. Chem. Chem. Phys.* **2005**, *7*, 1657.
(29) Deakin, J. J.; Husain, D. J. *J. Chem. Soc., Faraday Trans. II* **1972**, *18*, 1603.